INVESTIGATION OF MAGNETIC PROPERTIES OF 0.10 MM AND 0.23 MM ORIENTED SILICON STEEL UNDER DIFFERENT OPERATING CONDITIONS

Yu HAN[1], Yang LIU[2*], Fuyao YANG[3], Hongwei XIE[4], Baozhi LIU[5], Jie GAO[6]

With the different supply waveforms, different types of oriented silicon steel have different magnetic properties in power electronics. In this paper, the magnetic properties of 0.10 mm- *and 0.23 mm-oriented silicon steels under different operation conditions were measured based on medium-frequency Epstein frame. The variation laws of magnetic properties of the above materials were revealed. Some suggestions on selection of oriented silicon steels were proposed through comparison of their magnetic properties under different frequency sine magnetizations, pulse width modulation (PWM) magnetization, and special pulse magnetization. Research conclusions provide data supports to the design of power electronics.*

Keywords: power electronics, different operation conditions, oriented silicon steel, magnetic properties

1. Introduction

Currently, power electronics are extensively applied to various fields, such as direct current (DC) transmission, flexible alternating current (AC) transmission, and rail traffic [1-3]. With large-scaled applications of power electronic devices, operation conditions of electrical equipment become more complicated. The electrical equipment usually works in environment with high temperature rise and under medium-high frequency non-sine excitation conditions [4-6]. The oriented silicon steel is a common soft magnetic material in electrical

[1] Prof. S. E., State Grid Smart Grid Research Institute Co. Ltd, State Key Laboratory of Advanced Power Transmission Technology, Beijing, China. e-mail: epri313@sina.com
[2] S. E., State Grid Smart Grid Research Institute Co. Ltd, State Key Laboratory of Advanced Power Transmission Technology, Beijing, China. e-mail: liuyang_white@hotmail.com
[3] S. E., State Grid Smart Grid Research Institute Co. Ltd, State Key Laboratory of Advanced Power Transmission Technology, Beijing, China. e-mail: yfyhit@163.com
[4] Eng. Xing'an power supply company of State Grid Inner Mongolia East Power Co., Ltd, Ulanhot, Inner Mongolia, 137499, China. e-mail: 616160571@qq.com
[5] Eng., Baotou Weifeng Rare Earth Electromagnetic Materials Co. Ltd, Baotou, Inner Mongolia, 014060, China. e-mail: 285626410@qq.com
[6] S. E., State Grid Smart Grid Research Institute Co. Ltd, State Key Laboratory of Advanced Power Transmission Technology, Beijing, China. e-mail: 330630508@qq.com

equipment. The magnetic properties of oriented silicon steel under operation conditions influences safety and reliability of electrical equipment directly [7].

Generally, the oriented silicon steel can be divided into two types based on its thickness. One is ultrathin oriented silicon steel with a thickness smaller than or equal to 0.10 mm. The other is an ordinary oriented silicon steel with thickness higher than or equal to 0.20 mm (non-laser notch type) [8]. At present, the ordinary oriented silicon steel has been widely applied, and some data on magnetic properties under different operation conditions have been accumulated. In [9]-[14], the magnetic loss of laminated steel was measured under various temperatures and frequencies by using the Epstein frame. In [15] and [16], an automatic measurement system of iron loss of non-oriented silicon steel under PWM power excitation was built using the inverter circuit. In [17], a measuring method and a calculation model of silicon steel magnetic properties under PWM excitation were presented. In [18], the iron core test platform was built, and the effects of different harmonics on iron loss were investigated. Although these studies involved measurement of silicon steel properties under different operating conditions, they focus on ordinary oriented silicon steel or non-oriented silicon steel. None of them discussed the magnetic properties of ultrathin oriented silicon steel. Therefore, designers of power electronics are confused in selecting ultrathin oriented silicon steel or ordinary oriented silicon steels.

Based on previous studies, this paper measures magnetic properties of 0.10 mm- and 0.23 mm-oriented silicon steels under different operation conditions by using the medium-frequency Epstein frame. The magnetic properties of the above steels under sine magnetization, PWM excitation, and special pulse conditions were compared. Results provide data supports for the design and type selection of iron core materials of power electronics.

2. Measurement method

2.1 Medium-frequency Epstein frame

The traditional Epstein frame is a relatively mature way to measure magnetic properties of magnetic materials. Its highest test frequency is 400 Hz [19]. To measure magnetic properties under medium-frequency and high-flux density conditions, the traditional Epstein frame with 700 turns was improved, and a medium-frequency Epstein frame measuring device was developed. The primary and secondary coils decreased by 100 turns to increase the measured frequency to be higher than 1 kHz. The improved medium-frequency Epstein frame satisfies regulations in IEC 60404-10 standard. The schematic and physical image of medium-frequency Epstein frame measurement device is shown in Fig. 1.

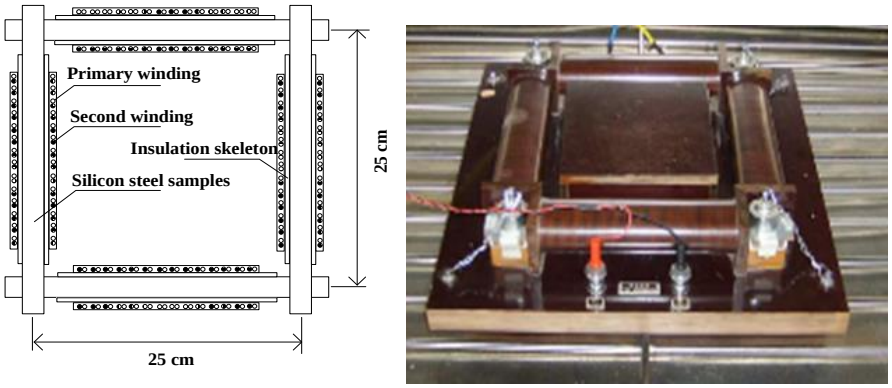

(a) Schematic (b) Physical image

Fig. 1. Medium-frequency Epstein frame measurement device

2.2 Implementation methods under different operation conditions

During measurement of magnetic properties, a voltage signal is produced through the analog output port of the computer-controlled data acquisition card. This voltage signal provides excitation voltage to the primary coil of the Epstein frame after passing through the power amplifier and isolation transformer. The analog input port of the data acquisition card is applied to collect current of the primary winding and voltage of the secondary coil to measure magnetic field intensity (**H**) and magnetic flux density (**B**). The computer corrects the analog output voltage signal continuously according to the difference between magnetic flux density (**B**) waveforms collected every time and the target magnetic flux density waveform (control objective) until reaching consistency. The waveform control method [17] is expressed as follows:

$$U_{out}^{(i+1)} = U_{out}^{(i)} + \frac{k(B_{target} - B_{measure}^{(i)})}{B_{target}} U_{out}^{(i)} \tag{1}$$

where i is the number of iterations, k is the proportional coefficient, U_{out} is the output voltage waveform, B_{target} is the target flux density waveform, and $B_{measure}$ is the magnetic flux density waveform gained according to the integral of the secondary-induced voltage. The target magnetic flux density waveform can be either sine wave or non-sine wave, and it is set by the measuring staff based on excitation conditions of real power electronics. In this paper, the magnetic flux density B is controlled by the adaptive program during all the measurements.

2.3 Determination of magnetic loss

According to the secondary voltages of the Epstein frame, the instantaneous magnetic flux density can be expressed as follows:

$$B(j) = -\frac{1}{N_2 A_s n f} \sum_{k=1}^{j} [U_2(k) + U_2(k+1)]/2 \quad (2)$$

where j is an integer, n is the number of sampling points in one period, f is the magnetizing frequency, N_2 is number of turns of the secondary winding.

- The magnetic field intensity can be expressed as follows:

$$H(j) = \frac{N_1}{l_{eff}} I(j) \quad (3)$$

where l_{eff} is the effective magnetic circuit length, N_1 is number of turns of the primary winding, I is the primary winding current.

The magnetic loss including eddy currents losses, hysteresis losses and excess losses, can be calculated as follows:

$$P = -\frac{N_1}{n\rho_m N_2 A_s l_{eff}} \sum_{j=1}^{n} U_2(j) \cdot I(j) \quad (4)$$

where ρ_m is the material density, A_s is the effective cross-sectional area.

3. Comparative analysis of magnetic properties of 0.10 mm- and 0.23 mm-oriented silicon steels

To avoid confusion of designers in selecting ultrathin and ordinary-thickness oriented silicon steels, the GT100 (0.10 mm) and 23QG100 (0.23mm) ordinary-thickness oriented silicon steels are measured with medium-high-frequency sine magnetization, PWM, and special pulse oscillation.

3.1 Magnetic properties under conditions of sine magnetization

In the measurement, the sinusoidal flux density B was applied as magnetization conditions. The magnetizing curves of GT100 (0.10mm) and 23QG100 (0.23mm) with different frequencies were given in Fig. 2.

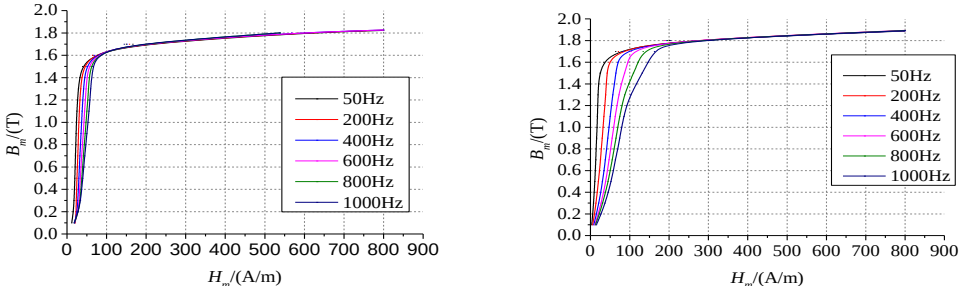

(a) GT100 (b) 23QG100

Fig. 2. Magnetizing curves with different frequencies

It can be seen from Fig.2 that the supplied frequency affects the saturated regional magnetizing curves of the two oriented silicon steels slightly. The

magnetizing curves after saturation overlap under different frequencies. Prior to saturation, the magnetizing curves are relatively sensitive to frequency variation. With the frequency increase, the magnetic permeability declines gradually. Compared with the ultrathin oriented silicon steel, the magnetic permeability of the ordinary-thickness steel decreases remarkably with the increase in frequency, and it is considerably influenced by frequency. The relative magnetic permeability of GT100 and 23QG100 oriented silicon steels under different frequencies with B_m=1.50T are shown in Table 1. As the frequency increases from 50 Hz to 1000 Hz, the relative magnetic permeability of the ultrathin oriented silicon steel decreases by 39%, whereas the relative magnetic permeability of the ordinary-thickness oriented silicon steel decreases by 81%.

Table 1

Relative permeabilities **of GT100 and 23QG100 oriented silicon steels at B_m=1.5 T**

Model No.	50 Hz	400 Hz	600 Hz	1000 Hz
GT100	30239	23817	21580	18402
23QG100	49006	18504	13757	9084

The loss curves of GT100 and 23QG100 oriented silicon steels with frequency changes are compared in Fig. 3. According to comparison results, the GT100 and 23QG100 oriented silicon steels have different frequency application ranges and critical loss frequencies.

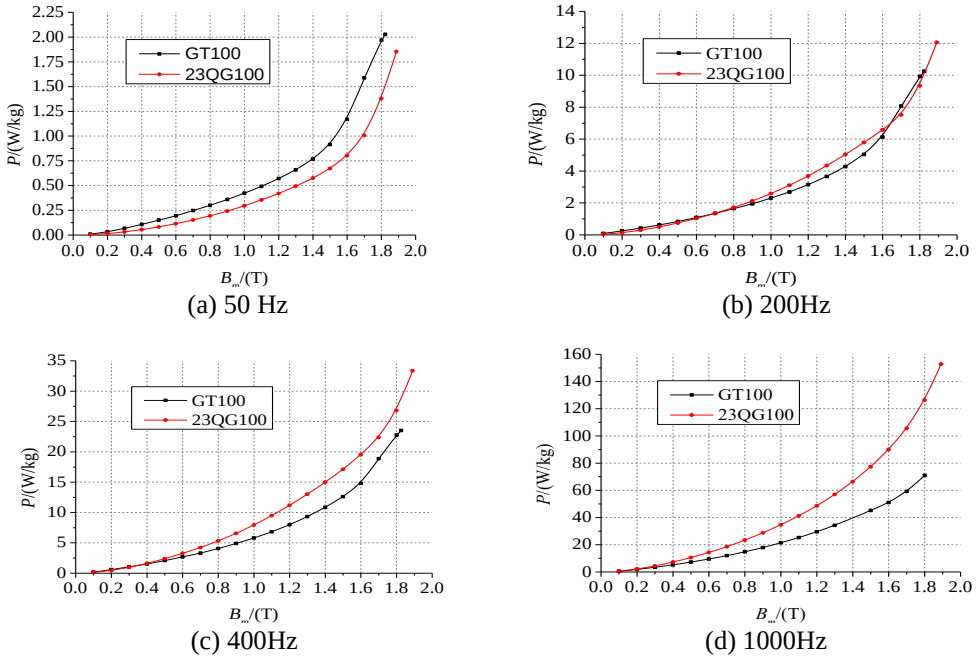

(a) 50 Hz (b) 200Hz

(c) 400Hz (d) 1000Hz

Fig. 3. Loss curves of GT100 and 23QG100 oriented silicon steels with frequency changes

For GT100 and 23QG100 oriented silicon steels, the critical frequency of loss is around 200 Hz. When the frequency is lower than 200 Hz, the 23QG100 oriented silicon steel has specific lower loss. When the frequency is higher than 200 Hz, the GT100 oriented silicon steel has lower specific loss. Therefore, given the different model number of silicon steel, the critical frequencies of loss of GT100 and 23QG100 oriented silicon steels may change. Hence, the oriented silicon steels of different model number should be further tested and analyzed to determine the relevant critical frequencies of loss.

3.2 Magnetic properties under PWM condition

The PWM has been extensively used in power electronics. It can be divided into unipolar and bipolar types according to modulation mode. The bipolar PWM waveforms are shown in Fig. 4. Sine wave (U_r) and triangular wave (U_c) are the modulating and carrier signals, respectively, and U_o is the output equivalent pulse voltage. In PWM, two factors influencing output voltage are carrier wave ratio and modulation ratio. The carrier wave ratio can be expressed as follows:

$$K_f = \frac{f_v}{f_s} \tag{5}$$

where K_f is the carrier wave ratio, f_v is the carrier frequency, and f_s is the modulation frequency.

The modulation ratio can be expressed as follows:

$$K_A = \frac{U_{rm}}{U_{cm}} \tag{6}$$

where K_A is the modulation ratio, U_{rm} is the amplitude of modulation wave, and U_{cm} is the amplitude of carrier wave.

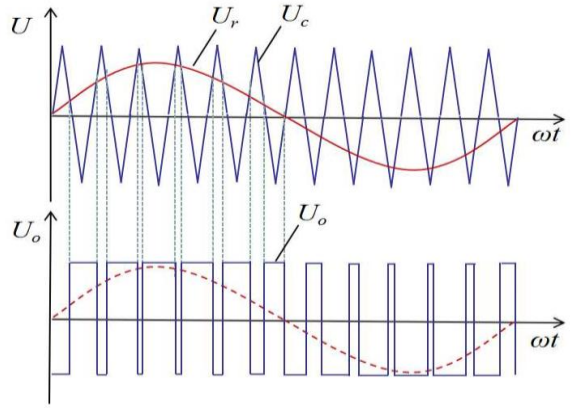

Fig. 4. Bipolar PWM waveforms

The magnetic properties of GT100 and 23QG100 oriented silicon steels under bipolar PWM were analyzed in this section. In the measurement, the

magnetic flux density B corresponding to the PWM voltage was applied as magnetization conditions. The influences of carrier ratio on the magnetic hysteresis loop of the GT100 oriented silicon steel when K_A=0.9 and f_s=50 Hz are shown in Fig. 5. The influences of carrier ratio on loss curves of the GT100 oriented silicon steel are shown in Fig. 6.

With the increasing carrier ratio, the magnetic flux density and harmonic components in magnetic field intensity decrease, whereas the harmonic number increases. The area of local magnetic hysteresis loop in the magnetic hysteresis loop decreases gradually, accompanied with a gradual reduction trend of loss.

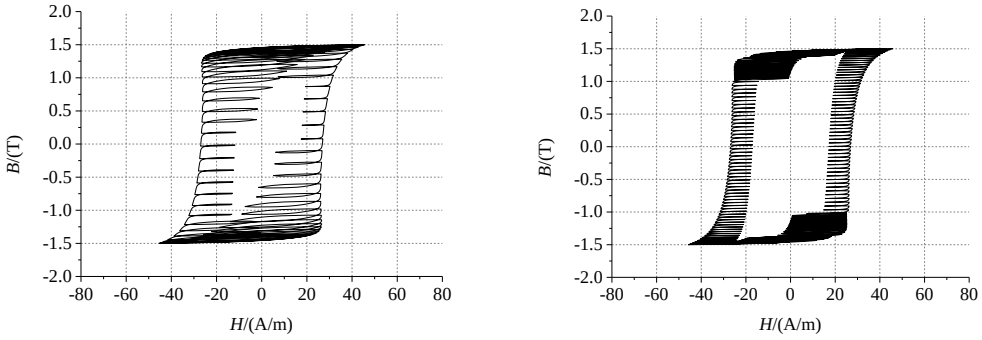

(a) K_f=60 (b) K_f=100

Fig. 5. Influences of carrier ratio on magnetic hysteresis loop of GT100 when K_A=0.9

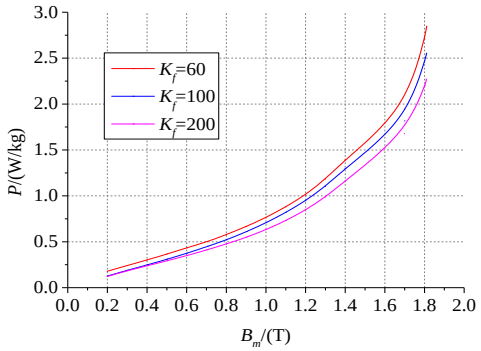

Fig. 6. Influences of carrier ratio on loss curve of GT100 oriented silicon steel when K_A=0.9

The influences of modulation ratio on magnetic hysteresis loop of the GT100 oriented silicon steel when K_f=60 and f_s=50 Hz are shown in Fig. 7. The influences of modulation ratio on loss curves of the GT100 are given in Fig. 8. With the reduction of modulation ratio, the area of local magnetic hysteresis loop in the magnetic hysteresis loop increases gradually, accompanied with a gradual increasing trend of loss.

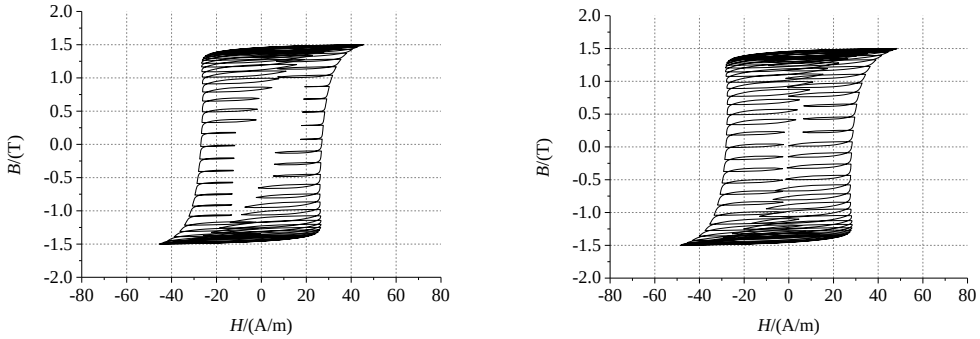

(a) K_A=0.90 (b) K_A=0.75

Fig. 7. Influences of modulation ratio on magnetic hysteresis loop of GT100 when K_f=60

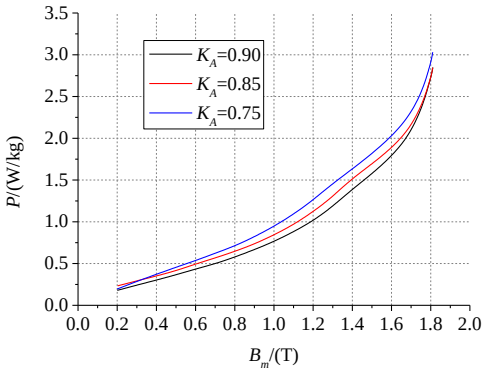

Fig. 8. Influences of modulation ratio on loss curve of GT100 when k_f=60

Influence of modulation ratio and carrier ratio on magnetic hysteresis ratio and loss characteristics of the GT100 and 23QG100 oriented silicon steels are same. Therefore, in this paper, the measuring results of the magnetic properties of the 23QG100 with different modulation ratios and carrier ratios were omitted.

Comparison of the loss curves of GT100 and 23QG100 oriented silicon steels under different modulation wave frequencies when K_A=0.9 and K_f=60 is given in Fig. 9. It is obvious that with the same modulation ratio and carrier ratio, the losses of GT100 and 23QG100 oriented silicon steels are mainly related with modulation frequency. With the increase of modulation frequency, the core loss of 23QG100 increases, but core loss of the GT100 is relatively lower. Based on the above analysis, if the same modulation ratio and carrier ratio are given, the oriented silicon steel type should be selected according to the modulation wave frequency. When the modulation wave frequency is high, the GT100 oriented silicon steel is the first option.

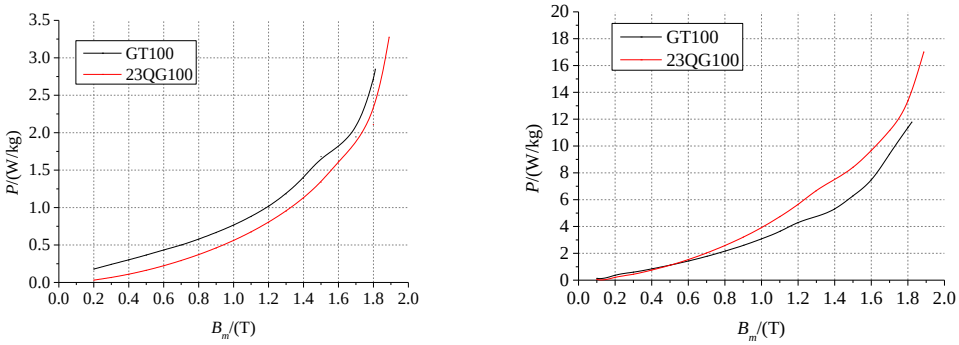

(a) f_s=50 Hz (b) f_s=200 Hz

Fig. 9. Comparison of loss curves of GT100 and 23QG100 under different carrier frequencies when K_A=0.90 and K_f=60

When the modulation wave frequency is low, the 23QG100 oriented silicon steel shall be selected.

3.3 Magnetic properties under special pulse oscillation

At present, the magnetic properties of oriented silicon steels under such special operation conditions have not been reported yet. In this paper, the magnetic properties of GT100 and 23QG100 oriented silicon steels under operation conditions of saturation resistor of the ultrahigh voltage DC converter valve were compared and analyzed.

The voltage waveform of saturation resistor of the ultrahigh voltage DC converter valve in one time period is shown in Fig. 10. In one time period, the valve is opened positively once and cut off inversely once, forming special impulse oscillation conditions.

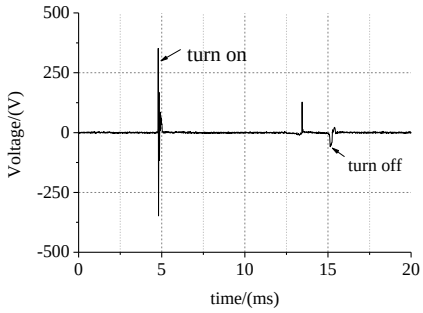

Fig. 10. Voltage waveform of saturation resistor of ultrahigh voltage DC converter valve

In the measurement, the magnetic flux density B corresponding to the special impulse oscillation voltage was applied as magnetization conditions. The measured magnetic properties of GT100 and 23QG100 oriented silicon steels under pulse oscillation at B_m=1.80T are given in Fig. 11. It shows that under such

unique working conditions, the flux density waveform and magnetic field intensity have serious distortions. The magnetic hysteresis loop has many complicated local magnetic hysteresis loops.

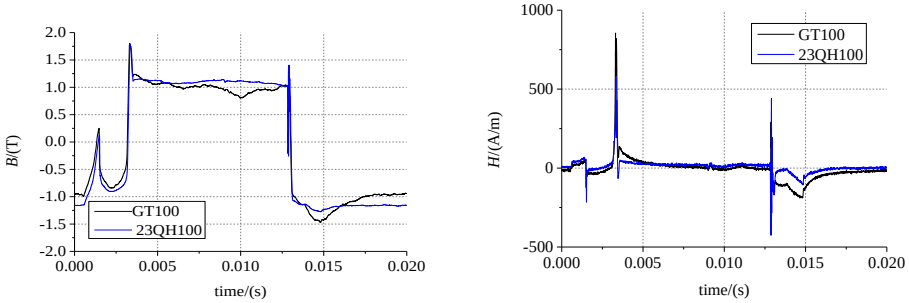

(a) Flux density (b) Field intensity

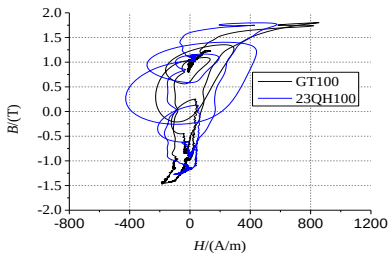

(c) Hysteresis loop

Fig. 11. Measured magnetic properties of GT100 and 23QG100 under continuous pulse oscillation when B_m=1.80 T

The loss curves of GT100 and 23QG100 under special pulse oscillation are compared in Fig. 12. According to comparison results, the 23QG100 has evident losses. The magnetic properties of 23QG100 under high frequency are relatively poor and the area of hysteresis loop is relatively large given the short pulse oscillation period and high-frequency effect.

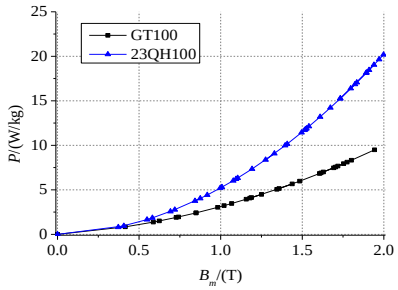

Fig. 12. Measured loss curves of GT100 and 23QG100 oriented silicon steels under pulse oscillation

4. Conclusions

Based on the improved Epstein frame, the magnetic properties of GT100 and 23QG100 oriented silicon steels under different operation conditions are measured and investigated in this paper, the following conclusions are obtained:

(1) With sine wave magnetization, the critical frequency of loss of GT100 and 23QG100 oriented silicon steels is 200 Hz. When the frequency is lower than 200 Hz, the 23QG100 oriented silicon steel has high magnetic permeability and low magnetic loss. Otherwise, the magnetic permeability and loss of the 23QG100 oriented silicon steel decrease significantly. The GT100 oriented silicon steel shows better magnetic permeability and magnetic loss.

(2) With PWM, the variation of the magnetic properties of GT100 and 23QG100 are the same. The magnetic loss is negatively related with carrier ratio with the same modulation ratio, but it is negatively related with modulation ratio with the same carrier ratio.

(3) With the same PWM condition, the GT100 oriented silicon steel is better under high modulation wave frequency. The critical frequency of loss of GT100 and 23QG100 oriented silicon steels under PWM is lower than that under sine magnetization at different frequencies (200 Hz). Under special excitation conditions with characteristic of high-frequency magnetization, the GT100 oriented silicon steel has evident advantages.

R E F E R E N C E S

[1] K. -i. Yamashita, G. Tsukamoto and S. Nishikata, "Steady-State Characteristics of a Line-Commutated Converter-Based High-Voltage Direct Current Transmission System for Series-Connected Wind Power Plants," IEEE Transactions on Industry Applications, vol. 56, no. 4, pp. 3932-3939, July-Aug. 2020.

[2] Y. Wan, M. A. A. Murad, M. Liu and F. Milano, "Voltage Frequency Control Using SVC Devices Coupled With Voltage Dependent Loads," IEEE Transactions on Power Systems, vol. 34, no. 2, pp. 1589-1597, March 2019.

[3] J. Fabre, P. Ladoux, H. Carcon, A. Verdcchio, J.-M. Blaquiere, D. Flumian, and S. Sanchez., "Characterization and Implementation of Resonant Isolated DC/DC Converters for Future MVdc Railway Electrification Systems," IEEE Transactions on Transportation Electrification, vol. 7, no. 2, pp. 854-869, June 2021.

[4] H. S. Zhao, H. H. Eldeeb. Y. L. Zhang, D. D. Zhang, Y. Zhan, G. R. Xu, and O. A. Mohammed, "An Improved Core Loss Model of Ferromagnetic Materials Considering High-Frequency and Nonsinusoidal Supply," IEEE Transactions on Industry Applications, vol. 57, no. 4, pp. 4336-4346, July-Aug. 2021.

[5] C. Wang, C. Tian, H. Cheng and J. Deng, A PWM Method of H-Bridge Converter with Temperature Rise Balancing and Minimization Based on Periodically Alternating Employment of Power Devices, IEEE Transactions on Power Electronics, vol. 37, no.9, pp.11135-11151, Sept. 2022

[6] E. Cazacu, L. Petrescu and V. Ioniţă, Losses and Temperature Rise Within Power Transformers Subjected to Distorted Currents, 2017 15th International Conference on Electrical Machines, Drives and Power Systems (ELMA), 2017, pp. 362-365.
[7] X. Zhao, X. Liu and L. Li, Hysteretic and Loss Modeling of Silicon Steel Sheet under the DC Biased Magnetization Based on the Preisach Model, 2019 22nd International Conference on Electrical Machines and Systems (ICEMS), 2019, pp. 1-6.
[8] H. Toda, K. Senda, S. Morimoto and T. Hiratani, Influence of Various Non-Oriented Electrical Steels on Motor Efficiency and Iron Loss in Switched Reluctance Motor, IEEE Transactions on Magnetics, vol. 49, no. 7, pp. 3850-3853, July 2013.
[9] S. E. Zirka, Y. I. Moroz, P. Marketos, A. J. Moses, D. C. Jiles and T. Matsuo, Generalization of the Classical Method for Calculating Dynamic Hysteresis Loops in Grain-Oriented Electrical Steels, IEEE Transactions on Magnetics, vol. 44, no. 9, pp. 2113-2126, Sept. 2008.
[10] O. Stupakov, R. Wood, Y. Melikhov and D. Jiles, Measurement of Electrical Steels With Direct Field Determination, IEEE Transactions on Magnetics, vol. 46, no. 2, pp. 298-301.
[11] G. Shilyashki, H. Pfützner, E. Huber, G. Trenner and E. Gerstbauer, 3-D MACC Modeling of Instantaneous Magnetic Flux Distributions in Epstein Tester, IEEE Transactions on Magnetics, vol. 56, no. 9, pp. 1-5, Sept. 2020.
[12] M. L. Ababsa, O.Niet, G.Velu and J.P.Lecointe, High-Temperature Magnetic Characterization Using an Adapted Epstein Frame, IEEE Transactions on Magnetics, vol.54, NO.6, 2018.
[13] Z. Cheng, N. Takahashi, and B. Forghani et al, Modeling of Magnetic Properties of GO Electrical Steel Based on Epstein Combination and Loss Data Weighted Processing, IEEE Transactions on Magnetics, vol.50, NO.1, 2014.
[14] M. J. Manyage and P. Pillay, New Epstein frame for Core Loss Measurements at High Frequencies and High Flux Densities, in Proc. IEEE Ind. Appl. Soc. Annu. Meeting (IAS), Oct. 2008, pp. 1–6.
[15] H. Kaihara et al., Effect of Carrier Frequency and Circuit Resistance on Iron Loss of Electrical Steel Sheet Under Single-Phase Full-Bridge PWM Inverter Excitation, IEEE Transactions on Magnetics, vol. 48, no. 11, pp. 3454-3457, Nov. 2012.
[16] Junquan Chen, Weiming Ma, Dong Wang, Xiwen Yu and Yunjun Guo, Development of Automatic Iron Loss Measurement System of Magnetic Material with PWM Excitation, 2011 International Conference on Materials for Renewable Energy & Environment, 2011, pp. 1013-1017.
[17] IEC 62383, Determination of Magnetic Loss Under Magnetic Polarization Waveforms Including Higher Harmonic Components Measurement, Modelling and Calculation Methods, Geneva: IEC Central Office, 2006.
[18] M. Namikawa, H. Ninomiya, Y. Tanaka and Y. Takada, Magnetic Properties of 6.5% Silicon Steel Sheets under PWM Voltage Excitation, IEEE Transactions on Magnetics, vol. 34, no. 4, pp. 1183-1185, July 1998.
[19] Y. Li, X. Geng, C. Zhang, R. Yan and J. Zhu, "Improved 3-D Magnetic Properties Measurement of Silicon Steel Laminations Based on a Novel Sensing Structure," IEEE Transactions on Magnetics, vol. 53, no. 11, pp. 1-4, Nov. 2017.